CRYSTAL GROWTH & DESIGN

pubs.acs.org/crystal

Communication

Counterintuitive Crystallization: Rate Effects in Calcium Phosphate Nucleation at Near-Physiological pH

David P. McDonogh, Priyanthan Kirupananthan, and Denis Gebauer*

Cite This: *Cryst. Growth Des.* 2023, 23, 7037−7043

Read Online

ACCESS | Metrics & More | Article Recommendations | Supporting Information

ABSTRACT: Calcium phosphates are widely present in geological and industrial settings and make up the majority of our bone's inorganic content; however, their formation from solution is not fully understood. The nucleation of calcium phosphate phases was studied using a state-of-the-art titration setup. The effect of varied calcium addition rate was studied at a range of pH values between pH 7 and pH 8; the precipitated crystals were isolated and analyzed. Dicalcium phosphate dihydrate (DCPD) was formed at lower pH and a slow addition rate. Intermediate addition rates yielded a mix of DCPD and poorly crystalline hydroxyapatite (PC-HA). At fast addition rates and above pH 7.5, poorly crystalline hydroxyapatite was precipitated exclusively. The results indicate that counterintuitive kinetic effects play a substantial role in the nucleation of calcium phosphates.

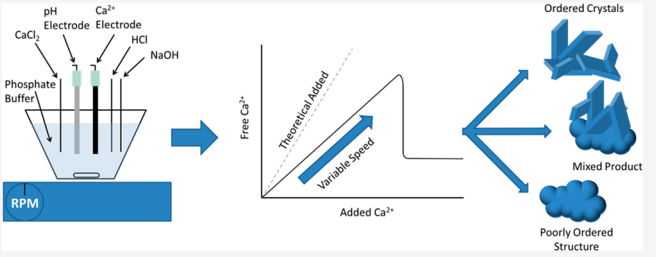

Although the nucleation, precipitation, and transformation of the calcium phosphate (CaP) phases have been extensively investigated since at least the 1960s, research continues to this day in order to fully understand these mechanisms.[1−5] The multitude of crystal structures, strong pH dependency, convolution of thermodynamic with kinetic factors, and debate about the composition of phases have made a comprehensive mechanism elusive. The widespread occurrence of calcium phosphate, in both natural (bones, teeth, atherosclerotic plaque) and industrial (fertilizer, catalysis, wastewater, dairy, food additive) contexts, give this field a high research priority.[4,6−9]

Due to the complexity of the calcium phosphate system, especially regarding its biological relevance, currently several approaches are used to study the formation of CaP phases. Pouring together two solutions, one containing phosphate ions and the other calcium, is the most direct method of precipitating solids from these species. This simple yet effective method has been used by multiple authors to screen the properties and transformation behavior of numerous substituted amorphous calcium phosphate (ACP) samples.[10,11] Slower, more controlled addition can be used for similar substitutional screening of a desired crystal polymorph as done by Boanini et al. with dicalcium phosphate dihydrate (DCPD).[12] Premixing the reagents at low pH and driving the reaction with ammonia diffusion−similar to methods established for mineral systems−has also found popularity in biologically inspired studies.[13−15] Furthermore, double diffusion methods employing permeable gels or membranes, where the mixing rate is significantly reduced, have also found application to study Liesegang patterns and growth in confined spaces.[16−18] Calcium diffusion into phosphate has also been used to grow macroscopic, complex shaped crystals in chemical garden systems.[19,20]

The studies above mainly focused on producing solid phases to analyze their properties or to look at later transformation processes. In situ pH measurements, on the other hand, allow the nucleation and transformation to be observed starting from start to finish from ions in solution to stable precipitated phases. Multiple authors have used such methods, observing several stages in the pH evolution beginning with the formation of ion pairs and various ACP types, followed by intermediate phases before seeing transformation into and the growth of hydroxyapatite (HA).[21,22] The existence and transformation of multiple ACP phases (ACP1 and ACP2) controlled via solution-mediated processes was introduced by Christoffersen using similar methods more than 30 years prior.[23] The presence of additives in these experiments often inhibits nucleation and stabilizes intermediates; however, the pH measurements show the same general features.[24,25] The various stages seen in solution can also be sampled; transmission electron microscopy (TEM) shows a progression from globular amorphous particles to structured crystals.[22,25] Further progress with in situ measurements has been made by Hoeher et al.; using a flow reactor, they were able to couple pH measurement with scattering techniques, and it could be

Received: July 19, 2023
Revised: September 19, 2023
Published: September 25, 2023

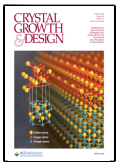

https://doi.org/10.1021/acs.cgd.3c00851
Cryst. Growth Des. 2023, 23, 7037−7043

shown that the initial calcium-to-phosphate ratio in solution determined the extent of monodentate or bidentate binding between the ions, which, in turn, influences the final polymorph produced.[26] In situ Raman spectroscopy has also been coupled with pH measurements to observe the transformation of ACP to HA.[27]

Similarly, the improvements in liquid cell and in situ TEM methods from the past few years have allowed the direct observation of nucleating crystals. Jin and co-workers explicitly investigated the transformation of amorphous calcium phosphate into HA; from their observations, they suggest that, while HA nucleates spontaneously in solution, transformation of large ACP nanoparticles providing surface nucleation sites for HA is another key mechanism.[28] Other groups have also confirmed the importance of ACP in in situ TEM studies. Dalmonico et al. suggested that multiple mechanisms exist, seeing two types of ACP followed by growth driven by addition of ions or nanoclusters, or ACP nanoparticles either aggregating or attaching to previously nucleated HA.[29] Other authors have also supported the possibility of multiple nucleation mechanisms coexisting, declaring that both classical and nonclassical nucleation pathways exist in liquid cell TEM.[30] Furthermore, this work showed a surface nucleation of HA on ACP particles.[30]

While the methods mentioned above provide direct access to processes happening in solution, the reaction conditions are uncontrolled. Buffer capacity of additives, for example, may cover up pH effects, while TEM measurements can suffer from confinement effects and damage due to the high beam energy. A controlled mineralization procedure was first developed for calcium carbonates; a calcium solution is slowly added to carbonate buffer while NaOH is used to maintain a constant pH value.[31] This titration method allows detailed observation of the calcium concentration in solution through an ion-selective electrode; the amount of base used indirectly describes the amount of counterions consumed and shifts in speciation. The resulting titration curves have a linear prenucleation regime where the calcium concentration in solution rises, a sharp drop in concentration occurs at nucleation before a solubility plateau is established after the final stable phase is formed.[32] Such experiments allow detailed study along the entire nucleation pathway and have led to the discovery of previously overlooked aspects in calcium carbonate nucleation.[33] Investigations with additives and adaption to other chemical systems have shown how versatile this method is.[34−38]

Several works have used this titration method to re-examine the mechanisms behind calcium phosphate nucleation. Carino et al. focused on physiological conditions (pH 7.4, T = 37 °C), developing a thermodynamic-kinetic model based on measurements at various ionic strengths.[39] Both Ibsen et al.[40] and Ruiz-Agudo et al.[41] investigated additive effects at pH 8, using osteopontin and citrate, respectively, as model substances. Both works saw a delay in nucleation alongside definite kinks in the titration curves, indicating that stabilized intermediate species were formed, which was postulated to be a liquid precursor.[40,41] In this work, we see a counterintuitive effect of the calcium addition rate on the titration, indicating that alongside pH, temperature, concentration, etc., counter-intuitive kinetic factors are key in the nucleation of CaP phases. This correlates well with the complicated nature of this system, which has led to considerable debate about the mechanisms of formation and even composition of the solid precipitates, as described in a recent review.[3]

In our study, a calcium containing solution (5 mM) was added to a phosphate buffer (10 mM) maintaining a constant pH value with NaOH (0.1 M); the addition rate was varied from 0.01 to 1.00 mL/min (see the Experimental Section in the Supporting Information for details). The procedure was adapted from other chemical systems; the chosen concentrations were found to allow for nucleation to occur within the addition period. As can be seen in Figure 1, there is a linear

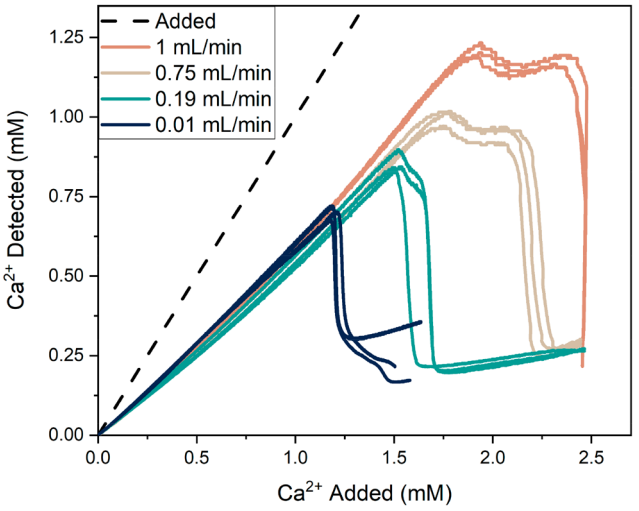

Figure 1. Selection of titration curves at pH 7.3, illustrating the changes seen as the addition rate is increased. The development of the plateaus and extension of the prenucleation regime are evident. Data collection ends at an added Ca^{2+} concentration near 2.5 mM for the fast dosing rates as the reaction vessel is full (see Figure S2 for time-based plots and Figures S3−S7 in the Supporting Information for a comparison of nucleation events). The final plateau is well-defined for fast addition rates; however, some variability is seen at intermediate addition rates. Slow addition rates also show differing behavior in the final free Ca^{2+} concentration.

increase of Ca^{2+} ions in solution; the slope is identical at all dosing speeds (see Figure S1 in the Supporting Information). The essentially linear nature of this prenucleation regime and the lack of significant deviations from the behavior observed at the slowest addition rate confirms that good mixing occurs across the range of addition speeds; insufficient mixing would result in nonlinear deviations. At higher addition rates, the prenucleation regime extends to higher amounts of added calcium until nucleation occurs. Post-nucleation slow and fast addition rate curves demonstrate clear differences; in the former, the nucleation occurs as expected, with the free calcium concentration falling precipitously before reaching a constant value. At higher speeds the free calcium concentrations plateaus shortly after nucleation, before a larger second drop brings the concentration to a final level comparable to that of the slower titrations (also see the time-based plots in Figure S2 in the Supporting Information).

Transitioning from slow to fast, the development of the plateau can be seen. Initially, this starts out as a small section post-nucleation with a gradual slope at 0.10 mL/min simultaneously increasing in duration and decreasing in slope as the addition rate is increased. Interestingly, the plateau does not evolve in a consistent manner, for addition rates between

https://doi.org/10.1021/acs.cgd.3c00851
Cryst. Growth Des. 2023, 23, 7037−7043

0.10 mL/min and 0.50 mL/min several sets of titrations show both curves both with and without a plateau or sloping regions post-nucleation (recall Figure S1). Additionally, there is a trend toward nucleation at higher added calcium concentrations for faster addition rates. This mirrors the effects of addition rate seen for the calcium carbonate, where faster additions are able to penetrate further into the binodal/spinodal gap, which is explained by the existence of thermodynamically stable ion associates as precursors to a mineral phase, instead of "classical" particles experiencing random fluctuations.[42] In the case here, a classical argument can also be made, since, at faster addition rates, there is less time for fluctuations to result in a critical nucleus before a certain supersaturation is reached. Due to unavoidable stochastic effects, however, there is some variation between addition rate and nucleation point (see Figure S2).

As seen in Figure 2, the final phase isolated from the titrations changes between rates of 0.10 and 0.20 mL/min. At

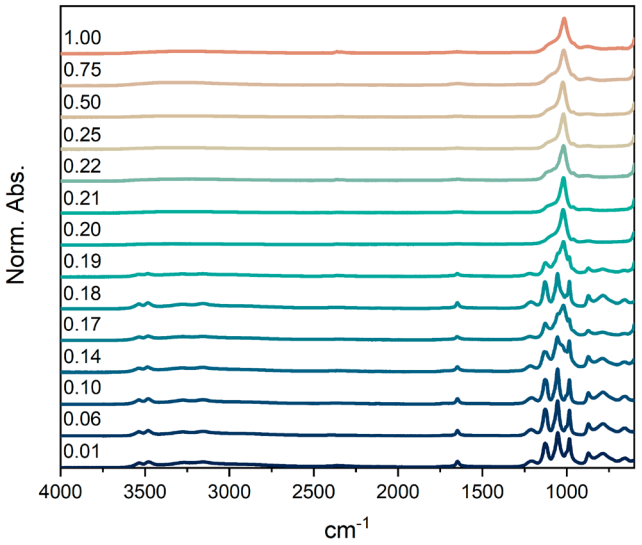

Figure 2. IR spectra of the isolated products at the end of the titrations for the indicated addition rates (mL/min) at pH 7.3. The transition from DCPD to PC-HA can be seen with a mix of products for rates between 0.10 and 0.21 mL/min. Peaks were assigned according to literature sources.[43−47]

low addition rates, the IR spectrum matches that of dicalcium phosphate dihydrate (DCPD); OH ν_1 and ν_3 stretching modes are signaled by bands at 3534, 3482, 3274, and 3154 cm^{-1}, the OH ν_2 deformation at 1723 and 1647 cm^{-1}, the P−OH ν_5 deformation at 1207 cm^{-1}, the phosphate ν_6 stretch at 1129 and 1055 cm^{-1}, the ν_2 phosphate symmetrical stretch at 984 cm^{-1}, the ν_3 phosphate at 872 cm^{-1}, the ν_5 deformation at 785 cm^{-1}, and finally the γ_{OH} libation at 656 cm^{-1}.[43,44] The IR spectra for high addition rates match that of poorly crystalline hydroxyapatite (PC-HA); between ∼3500 cm^{-1} and ∼3000 cm^{-1} a broad band and a smaller one at 1650 cm^{-1} are due to water in the isolated solids, the sharp peak at 1021 cm^{-1} contains the ν_3 signals from the phosphate, 960 cm^{-1} is the ν_1 signal, and 875 cm^{-1} is possibly due to the P−O(H) stretch or minor carbonate inclusion.[45−47] The P−O(H) stretch is possible as PC-HA may contain HPO_4^{2-} impurities within its structure; this is the dominant anion at the studied conditions.

The spectra obtained for the isolated end product at intermediate rates are a mixture of the spectrum seen at either extreme. In the IR spectra of the isolated solids at pH 7.3, from the addition rate of 0.14 mL/min until 0.19 mL/min, both DCPD and PC-HA are present. The fraction of PC-HA generally increases with addition rate—this can be seen more clearly in the XRD measurements, where DCPD is present even at 0.22 mL/min (Figure S8 in the Supporting Information). The broad PC-HA reflex at ∼32° 2θ increases with addition rate, while the reflexes from DCPD lose intensity before disappearing altogether. The IR spectra shown (Figure 2) do not align completely with the XRD results but show the same overall trend, progressing toward PC-HA with increased addition rate. There are small deviations, e.g., at 0.18 mL/min, the spectrum has more DCPD character than at 0.14 mL/min—this is likely due to the stochastic nature of nucleation, and particle size effects between the two methods.[48] Even with controlled quenching, the ratio of the two phases in the product isolated from the transition range varied; differences in the time between nucleation and isolation affect the composition of the final product. The exact composition of the mix, however, is not consequential; the existence of the transition region itself is the critical finding, as it provides direct insight into the nucleation mechanism (cf. below).

The addition rate effect can also be seen in the morphology of the isolated solids. As is evident in Figure 3, the mixed product obtained from midrange titration speeds (Figure 3a) has features of both the slow additions (Figure 3b) and fast addition rates (Figure 3c). At low addition speeds, joined platelets of different sizes are observed; at higher addition rates, agglomerates of shapeless rounded particles can be seen.

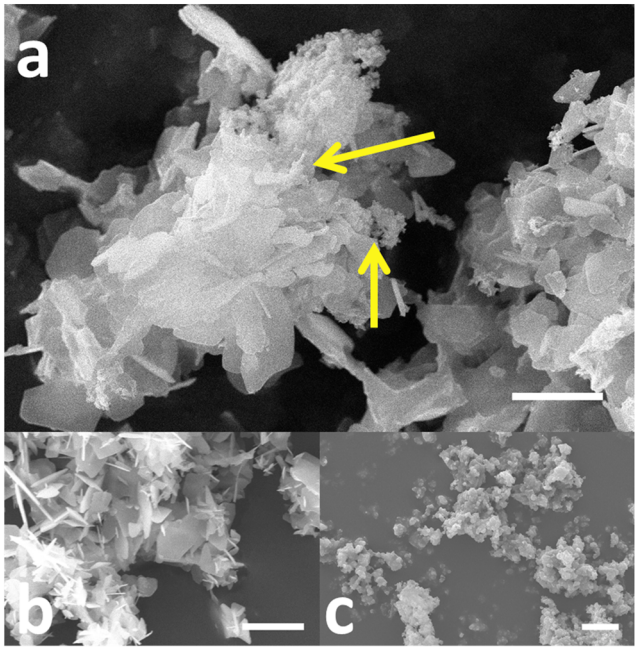

Figure 3. SEM images of products isolated from titrations at pH 7.3. (a) The mixed product (0.15 mL/min) shows similarities to both the platelets from the slow addition (panel (b), 0.01 mL/min) and the rounded shapeless aggregated particles at high addition rates (panel (c), 0.18 mL/min). Yellow arrows mark areas where DCPD and PC-HA coexist in the mixed product. Scale bars are 5, 10, and 30 μm in panels (a), (b), and (c), respectively.

https://doi.org/10.1021/acs.cgd.3c00851
Cryst. Growth Des. 2023, 23, 7037−7043

At the intermediate addition rate (Figure 3a), both motifs are present. The DCPD platelets tend to be more broken and less defined, while the PC-HA regions appear fluffier and more cloudlike (yellow arrows mark areas where the two phases coexist).

An increase of just 0.2 pH units to pH 7.5 results in PC-HA precipitating, even at the slowest addition rate of 0.01 mL/min (Figure 4). At pH 7.4, a mixed end product was seen between

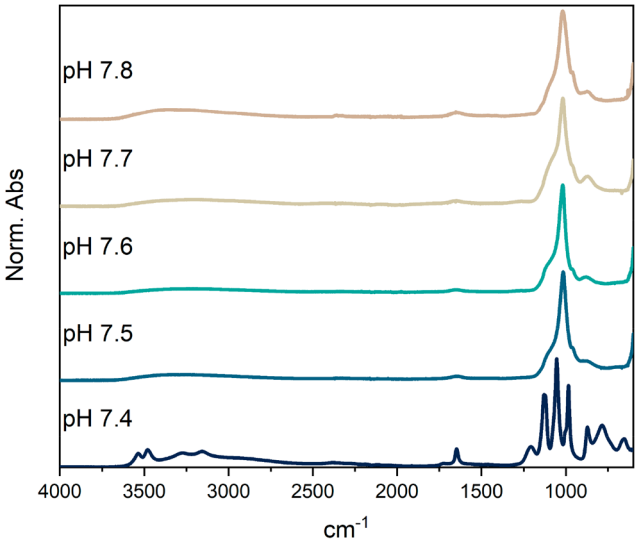

Figure 4. IR spectra of the isolated products at the end of the titrations for the indicated pH values at an addition rate of 0.01 mL/min. Above pH 7.4, PC-HA is produced instead of DCPD, even at this minimum titration rate. Peaks were assigned according to literature sources.[43−47]

0.13 mL/min to 0.18 mL/min, as shown in Figures S9−S11 in the Supporting Information. The coexistence of the two phases seems to be highly sensitive to pH; the transition region at pH 7.4 covers a range of 0.05 mL/min, compared to 0.12 mL/min at pH 7.3.

The nucleation of calcium phosphate is affected by kinetic influence, even at the low concentrations used in this work; the calcium addition rate determines the solid precipitated in solution. Surprisingly, a thermodynamically more stable product, PC-HA, is formed at higher addition rates, while a less-stable polymorph, DCPD, is formed at slow ones. It would be expected that gradually increasing the calcium concentration in solution would allow the thermodynamic product to form directly; however, this is not the case. Using a similar setup without pH control, DCPD was observed as the final product, even transforming from HAP, in more acidic conditions, between pH 5 and pH 6.[49] Earlier works, however, have yielded PC-HA at similar pH values, but amorphous calcium phosphate was used as a starting point.[50] This study shows that the discrepancy in the results is likely due to the complicated kinetic and thermodynamic relationships at near-neutral pH. Both the addition rate and pH were observed to influence the nucleation mechanism. Additionally, leaving a titration with addition rate 0.01 mL/min running for nearly 2 days did produce PC-HA as the final product, indicating that the thermodynamic product is indeed eventually formed, even at this pH. (See Figures S12 and S13 in the Supporting Information.) Such a long titration time is effectively comparable to incubating DCPD in a phosphate buffer—it is not unreasonable that a transformation to PC-HA eventually takes place, as has been observed previously.[26] The variation in the post-nucleation regime for titrations at 0.01 mL/min, however, suggests that more complex mechanisms underlie transformation, even under these conditions closest to thermodynamic equilibrium, i.e., the "reference" case for titration experiments.

Other works have observed DCPD and PCAA forming through octacalcium phosphate (OCP) and amorphous calcium phosphate (ACP) precursors, both under thermodynamically and kinetically controlled conditions.[51,52] These works, however, used much higher concentrations and faster addition rates, compared to those of the titrations above. This likely leads to kinetic influences affecting all experiments, as the nucleation is not completely under thermodynamic control, even under the experimental conditions described as thermodynamic by the authors. In this work, DCPD is seen to form directly at slow addition speeds. The bump, and eventual plateau in the titration curves at increased rates where PC-HA forms is likely due to the presence of an amorphous precursor species—attempts to isolate this from the titration only yielded PC-HA. Sampling using TEM reveals a progression in the species present in the plateau (see Figures S14 and S15 in the Supporting Information). In the titration, this possible precursor could be a transient species, coexisting with PC-HA in small amounts as it transforms. The more-soluble species then determines the solubility product in the titration, i.e., increased free calcium concentration, but not be present in quantities needed for analysis (or transform too quickly upon attempts toward isolation). Since quenching methods were not able to isolate the intermediate, advanced methods such as cryo-TEM to capture this phase as close to in situ are likely needed. Furthermore, the possibility that this transient species is only stable when in contact with the mother phase cannot be neglected—which would render isolation a moot point.[14,53]

The presence of different precursors means that the system is taking a different pathway when precipitating the final solid phase; the various experimental conditions lead to unique nucleation pathways. For both the calcium phosphates and carbonates, it has been shown that the initial solution stoichiometry is critical in determining the nucleation and growth processes, even when controlling other parameters.[26,54] The ratio of precursor ions in solution, at least in part, controls which nucleation mechanism is available. Such a result further underlines the complex nature of nucleation. This, together with the speed dependency seen in our titrations, indicates that kinetic barriers have an instrumental role in nucleation. Future work could further investigate the stoichiometric effects by either reversing the titration, adding phosphate buffer to a calcium solution, or the dual addition of calcium and phosphate into water. These changes would allow nucleation to be observed at different solution compositions.

Remarkably, the transition from DCPD to PC-HA at even the slowest addition rate occurs in a narrow pH range. Across all of the pH values studied, HPO_4^{2-} is the dominant phosphate species in solution, with $H_2PO_4^-$ being the only other species present in relevant concentrations. As seen in Figure S16 in the Supporting Information, the change in speciation from pH 7.4 to pH 7.5, the total amount of HPO_4^{2-} increases by only a few percent, while the amount of PO_4^{3-} is still well below 1%. Even though DCPD contains only calcium and HPO_4^{2-}, this shift to greater deprotonation of the

https://doi.org/10.1021/acs.cgd.3c00851
Cryst. Growth Des. 2023, 23, 7037−7043

phosphates is enough to completely surpass this polymorph. It must be noted that this occurs before HPO_4^{2-} reaches its maximum concentration in solution. We find it difficult to reconcile this with a purely thermodynamic pathway, as the solution environments between the two pH values are so similar. It seems more likely that a kinetic barrier is overcome for such a seemingly small change to influence the entire system to such a degree.

The effect of addition rate at the lower pH values further complicates the nucleation mechanism as there is no sharp transition between the initial formation of DCPD vs PC-HA, when increasing addition rate, indicating that there is a complex dependence on kinetic and thermodynamic factors, even under dilute conditions. Based on the addition rate of calcium, both DCPD and PC-HA could be isolated as products from the titration. Although it is not possible to unequivocally determine which phase forms first using our methods, we believe it to be reasonable that an amorphous precursor to PC-HA exists, possibly forming alongside DCPD once the addition rate is in the "transition region"; this precursor results in the "bump" and eventual plateau post-nucleation. The presence of amorphous precursors preceding the formation of PC-HA is supported by earlier works.[29] The "bump" strongly indicates that two phases are present due to its downward slope, which indicates a transformation is occurring; if one stable phase were present, then a definite plateau would be seen. It is possible that multiple processes are superimposed in such a manner; multimechanism pathways have been proposed previously for this system.[30]

Further investigation would be necessary to untangle the cocurrent mechanisms. The titration method can be modified to study the effects of varied calcium and phosphate concentrations, from Ca/P ratios of known phases to equal simultaneous additions or even to the extreme of titrating phosphate into calcium. Constant-composition experiments similar to those of Nancollas and co-workers can also be implemented, although Ca^{2+} addition would be used to trigger nucleation, instead of seed crystal addition.[55,56] Such adaptions would uncover the interplay of addition rate effects with stoichiometric ones, solution compositions are well-known to affect CaP nucleation.[23,26] While such experiments must certainly be carried out, we again highlight that the addition rate effect seen in this work occurs in CaP titration experiments, as they are currently performed by several research groups. The overview of the critical region provided here can help in further development of experimental methods, even before the processes behind the transition are fully understood.

As seen in the titrations here, multiple mechanisms would exist at addition rates between the two extremes, i.e., those where two distinct polymorphs are isolated together. Developing a complete mechanism that can account for such complex effects remains a challenge. In the classical view, the formation of the critical nucleus is considered the rate-determining step and the nucleation rate is calculated from the exponential of the change in free energy, the formation of PC-HA should be significantly faster than that of DCPD.[57,58] Additional statistical considerations reinforce the above points: the lower solubility of PC-HA means that higher supersaturation is achieved, compared to DCPD under the same solution conditions. Assuming the precritical nuclei for each species are independent, this means the precritical nuclei with PC-HA character must be both greater in number and be critical at a much smaller size. Taking a broader view and only considering the solubilities macroscopically, PC-HA should be nearly 50 orders of magnitude more likely to form.[59,60] While such an argument would also rationalize DCPD being more likely to form at higher addition rates as a higher concentration of Ca^{2+} is needed to reach a meaningful supersaturation of this phase, the isolation of mixed phases must still be reconciled.

A nonclassical nucleation model provides a framework to rationalize complex nucleation behavior as observed in this work; dynamic prenucleation species as described by the Prenucleation Cluster pathway may explain the behavior seen in the titrations.[61] While we cannot prove one mechanism here, our work clearly demonstrates that the calcium phosphate system shows surprising characteristics when applying state-of-the-art experimental methods. Previous works titrating CaPs have also seen complex behavior, with even ionic strength playing key role at otherwise tightly controlled experiments.[39−41] Here, we demonstrate that caution must be used in interpreting such studies, as the system does not behave in a predictable manner, indicating that further investigation is required until a complete understanding of CaPs can be developed. Understanding how small changes in conditions affect calcium phosphate nucleation is vital for developing a full mechanism of these minerals formation.

■ ASSOCIATED CONTENT

Supporting Information

The Supporting Information is available free of charge at https://pubs.acs.org/doi/10.1021/acs.cgd.3c00851.

Experimental details, additional titrations, titration comparison, XRD and additional IR spectra, SEM imaging for pH 7.4, phosphate speciation (PDF)

■ AUTHOR INFORMATION

Corresponding Author

Denis Gebauer − *Institute of Inorganic Chemistry, Leibniz University Hannover, D 30167 Hannover, Germany;* orcid.org/0000-0003-1612-051X; Email: gebauer@acc.uni-hannover.de

Authors

David P. McDonogh − *Institute of Inorganic Chemistry, Leibniz University Hannover, D 30167 Hannover, Germany;* orcid.org/0000-0002-6347-5914

Priyanthan Kirupananthan − *Institute of Inorganic Chemistry, Leibniz University Hannover, D 30167 Hannover, Germany*

Complete contact information is available at: https://pubs.acs.org/10.1021/acs.cgd.3c00851

Author Contributions

The manuscript was written through contributions of all authors. All authors have given approval to the final version of the manuscript.

Notes

The authors declare no competing financial interest.

■ ACKNOWLEDGMENTS

We would like to thank the cfMATCH analytics center at the Leibniz University Hannover for support and insight with the TEM measurements.

ABBREVIATIONS

CaP = calcium phosphate
ACP = amorphous calcium phosphate
HA = hydroxyapatite
TEM = transmission electron microscopy
DCPD = dicalcium phosphate dehydrate
PC-HA = poorly crystalline hydroxyapatite
OCP = octacalcium phosphate

REFERENCES

(1) Moreno, E.; Gregory, T.; Brown, W. Preparation and solubility of hydroxyapatite. *J. Res. Natl. Bur. Stand., Sect. A* **1968**, *72A* (6), 773.
(2) Marshall, R. W.; Nancollas, G. H. Kinetics of crystal growth of dicalcium phosphate dihydrate. *J. Phys. Chem.* **1969**, *73* (11), 3838−3844.
(3) Edén, M. Structure and Formation of Amorphous Calcium Phosphate and its Role as Surface Layer of Nanocrystalline Apatite: Implications for Bone Mineralization. *Materialia* **2021**, *17*, 101107.
(4) Wang, L.; Nancollas, G. H. Calcium orthophosphates: crystallization and dissolution. *Chem. Rev.* **2008**, *108* (11), 4628−4669.
(5) Garcia, N. A.; Malini, R. I.; Freeman, C. L.; Demichelis, R.; Raiteri, P.; Sommerdijk, N. A. J. M.; Harding, J. H.; Gale, J. D. Simulation of Calcium Phosphate Pre-Nucleation Clusters in Aqueous Solution: Association beyond ion pairing. *Cryst. Growth Des.* **2019**, *19*, 6422−6430.
(6) LeGeros, R. Z. Calcium Phosphate-Based Osteoinductive Materials. *Chem. Rev.* **2008**, *108*, 4742−4753.
(7) Kezia, K.; Lee, J.; Zisu, B.; Chen, G. Q.; Gras, S. L.; Kentish, S. E. Solubility of Calcium Phosphate in Concentrated Dairy Effluent Brines. *J. Agric. Food Chem.* **2017**, *65*, 4027−4034.
(8) Birkedal, H. *Phase transformations in calcium phosphate crystallization*. In *New Perspectives on Mineral Nucleation and Growth*; Springer, 2017; pp 199−210, DOI: 10.1007/978-3-319-45669-0_10.
(9) Van Driessche, A. E.; Kellermeier, M.; Benning, L. G.; Gebauer, D. *New Perspectives on Mineral Nucleation and Growth: From Solution Precursors to Solid Materials*; Springer, 2016.
(10) Yasar, O. F.; Liao, W.-C.; Stevensson, B.; Edén, M. Structural Role and Spatial Distribution of Carbonate Ions in Amorphous Calcium Phosphate. *J. Phys. Chem. C* **2021**, *125*, 4675.
(11) Sinusaite, L.; Kareiva, A.; Zarkov, A. Thermally induced crystallization and phase evolution of amorphous calcium phosphate substituted with divalent cations having different sizes. *Cryst. Growth Des.* **2021**, *21* (2), 1242−1248.
(12) Boanini, E.; Silingardi, F.; Gazzano, M.; Bigi, A. Synthesis and hydrolysis of brushite (DCPD): The role of ionic substitution. *Cryst. Growth Des.* **2021**, *21* (3), 1689−1697.
(13) Robin, M.; Tovani, C. B.; Krafft, J.-M.; Costentin, G.; Azaïs, T.; Nassif, N. The concentration of bone-related organic additives drives the pathway of apatite formation. *Cryst. Growth Des.* **2021**, *21* (7), 3994−4004.
(14) Gindele, M. B.; Steingrube, L. V.; Gebauer, D. Generality of liquid precursor phases in gas diffusion-based calcium carbonate synthesis. *CrystEngComm* **2021**, *23*, 7938.
(15) Chen, S.; Wang, Q.; Eltit, F.; Guo, Y.; Cox, M.; Wang, R. An ammonia-induced calcium phosphate nanostructure: a potential assay for studying osteoporosis and bone metastasis. *ACS Appl. Mater. Interfaces* **2021**, *13* (15), 17207−17219.
(16) Peters, F.; Epple, M. Simulating arterial wall calcification in vitro: biomimetic crystallization of calcium phosphates under controlled conditions. *Z. Kardiol.* **2001**, *90*, 81−85.
(17) Gebrehiwet, T.; Guo, L.; Fox, D.; Huang, H.; Fujita, Y.; Smith, R.; Henriksen, J.; Redden, G. Precipitation of calcium carbonate and calcium phosphate under diffusion controlled mixing. *Appl. Geochem.* **2014**, *46*, 43−56.
(18) Cantaert, B.; Beniash, E.; Meldrum, F. C. The role of poly (aspartic acid) in the precipitation of calcium phosphate in confinement. *J. Mater. Chem. B* **2013**, *1* (48), 6586−6595.
(19) Steenbjerg Ibsen, C. J.; Mikladal, B. F.; Bjørnholt Jensen, U.; Birkedal, H. Hierarchical tubular structures grown from the gel/liquid interface. *Chem. - Eur. J.* **2014**, *20* (49), 16112−16120.
(20) Hughes, E. A.; Robinson, T. E.; Moakes, R. J.; Chipara, M.; Grover, L. M. Controlled self-assembly of chemical gardens enables fabrication of heterogeneous chemobrionic materials. *Commun. Chem.* **2021**, *4* (1), 145.
(21) Xie, B.; Halter, T. J.; Borah, B. M.; Nancollas, G. H. Tracking amorphous precursor formation and transformation during induction stages of nucleation. *Cryst. Growth Des.* **2014**, *14* (4), 1659−1665.
(22) Habraken, W. J. E. M.; Tao, J.; Brylka, L. J.; Friedrich, H.; Bertinetti, L.; Schenk, A. S.; Verch, A.; Dmitrovic, V.; Bomans, P. H. H.; Frederik, P. M.; Laven, J.; van der Schoot, P.; Aichmayer, B.; de With, G.; DeYoreo, J. J.; Sommerdijk, N. A. J. M. Ion-association complexes unite classical and non-classical theories for the biomimetic nucleation of calcium phosphate. *Nat. Commun.* **2013**, *4*, 1507.
(23) Christoffersen, J.; Christoffersen, M. R.; Kibalczyc, W.; Andersen, F. A. A contribution to the understanding of the formation of calcium phosphates. *J. Cryst. Growth* **1989**, *94* (3), 767−777.
(24) Ding, H.; Pan, H.; Xu, X.; Tang, R. Toward a detailed understanding of magnesium ions on hydroxyapatite crystallization inhibition. *Cryst. Growth Des.* **2014**, *14* (2), 763−769.
(25) Ucar, S.; Bjørnøy, S. H.; Bassett, D. C.; Strand, B. L.; Sikorski, P.; Andreassen, J.-P. Formation of hydroxyapatite via transformation of amorphous calcium phosphate in the presence of alginate additives. *Cryst. Growth Des.* **2019**, *19* (12), 7077−7087.
(26) Hoeher, A. J.; Mergelsberg, S. T.; Borkiewicz, O. J.; Michel, F. M. Impacts of initial Ca/P on amorphous calcium phosphate. *Cryst. Growth Des.* **2021**, *21* (7), 3736−3745.
(27) Stammeier, J. A.; Purgstaller, B.; Hippler, D.; Mavromatis, V.; Dietzel, M. In-situ Raman spectroscopy of amorphous calcium phosphate to crystalline hydroxyapatite transformation. *MethodsX* **2018**, *5*, 1241−1250.
(28) Jin, B.; Liu, Z.; Shao, C.; Chen, J.; Liu, L.; Tang, R.; De Yoreo, J. J. Phase transformation mechanism of amorphous calcium phosphate to hydroxyapatite investigated by liquid-cell transmission electron microscopy. *Cryst. Growth Des.* **2021**, *21* (9), 5126−5134.
(29) Dalmônico, G. M.; Ihiawakrim, D.; Ortiz, N.; Barreto Junior, A. G.; Curitiba Marcellos, C. F.; Farina, M.; Ersen, O.; Rossi, A. L. Live Visualization of the Nucleation and Growth of Needle-Like Hydroxyapatite Crystals in Solution by In Situ TEM. *Cryst. Growth Des.* **2022**, *22* (8), 4828−4837.
(30) He, K.; Sawczyk, M.; Liu, C.; Yuan, Y.; Song, B.; Deivanayagam, R.; Nie, A.; Hu, X.; Dravid, V. P.; Lu, J.; et al. Revealing nanoscale mineralization pathways of hydroxyapatite using in situ liquid cell transmission electron microscopy. *Sci. Adv.* **2020**, *6* (47), eaaz7524.
(31) Gebauer, D.; Völkel, A.; Cölfen, H. Stable Prenucleation Calcium Carbonate Clusters. *Science* **2008**, *322* (5909), 1819−1822.
(32) Kellermeier, M.; Raiteri, P.; Berg, J. K.; Kempter, A.; Gale, J. D.; Gebauer, D. Entropy drives calcium carbonate ion association. *ChemPhysChem* **2016**, *17* (21), 3535−3541.
(33) Huang, Y.-C.; Rao, A.; Huang, S.-J.; Chang, C.-Y.; Drechsler, M.; Knaus, J.; Chan, J. C.; Raiteri, P.; Gale, J. D.; Gebauer, D. Uncovering the Role of Bicarbonate in Calcium Carbonate Formation at Near-Neutral pH. *Angew. Chem., Int. Ed.* **2021**, *60*, 16707.
(34) Verch, A.; Gebauer, D.; Antonietti, M.; Cölfen, H. How to control the scaling of $CaCO_3$: a "fingerprinting technique" to classify additives. *Phys. Chem. Chem. Phys.* **2011**, *13*, 16811−16820.
(35) Lukić, M. J.; Lücke, F.; Ilić, T.; Petrović, K.; Gebauer, D. On the Role of Poly-Glutamic Acid in the Early Stages of Iron (III)(Oxy)(hydr) oxide Formation. *Minerals* **2021**, *11* (7), 715.
(36) Ruiz-Agudo, C.; McDonogh, D.; Avaro, J. T.; Schupp, D. J.; Gebauer, D. Capturing an amorphous $BaSO_4$ intermediate precursor to Barite. *CrystEngComm* **2020**, *22* (8), 1310−1313.
(37) Wiedenbeck, E.; Kovermann, M.; Gebauer, D.; Cölfen, H. Liquid Metastable Precursors of Ibuprofen as Aqueous Nucleation Intermediates. *Angew. Chem., Int. Ed.* **2019**, *58* (52), 19103−19109.

https://doi.org/10.1021/acs.cgd.3c00851
Cryst. Growth Des. 2023, 23, 7037−7043

(38) Scheck, J.; Fuhrer, L. M.; Wu, B.; Drechsler, M.; Gebauer, D. Nucleation of hematite: A nonclassical mechanism. *Chem. - Eur. J.* **2019**, *25* (56), 13002−13007.
(39) Carino, A.; Ludwig, C.; Cervellino, A.; Müller, E.; Testino, A. Formation and transformation of calcium phosphate phases under biologically relevant conditions: experiments and modelling. *Acta Biomater.* **2018**, *74*, 478−488.
(40) Ibsen, C. J. S.; Gebauer, D.; Birkedal, H. Osteopontin Stabilizes Metastable States Prior to Nucleation during Apatite Formation. *Chem. Mater.* **2016**, *28*, 8550−8555.
(41) Ruiz-Agudo, E.; Ruiz-Agudo, C.; Di Lorenzo, F.; Alvarez-Lloret, P.; Ibañez-Velasco, A.; Rodriguez-Navarro, C. Citrate Stabilizes Hydroxylapatite Precursors: Implications for Bone Mineralization. *ACS Biomater. Sci. Eng.* **2021**, *7*, 2346.
(42) Avaro, J. T.; Wolf, S. L.; Hauser, K.; Gebauer, D. Stable Pre-nucleation Calcium Carbonate Clusters Define Liquid-Liquid Phase Separation. *Angew. Chem.* **2020**, *59*, 6155.
(43) Lu, B.-Q.; Willhammar, T.; Sun, B.-B.; Hedin, N.; Gale, J. D.; Gebauer, D. Introducing the crystalline phase of dicalcium phosphate monohydrate. *Nat. Commun.* **2020**, *11* (1), 1546.
(44) Berry, E.; Baddiel, C. The infra-red spectrum of dicalcium phosphate dihydrate (brushite). *Spectrochim. Acta, Part A* **1967**, *23* (7), 2089−2097.
(45) Wang, Y.; Chen, J.; Wei, K.; Zhang, S.; Wang, X. Surfactant-assisted synthesis of hydroxyapatite particles. *Mater. Lett.* **2006**, *60* (27), 3227−3231.
(46) Hutchens, S. A.; Benson, R. S.; Evans, B. R.; O'Neill, H. M.; Rawn, C. J. Biomimetic synthesis of calcium-deficient hydroxyapatite in a natural hydrogel. *Biomaterials* **2006**, *27* (26), 4661−4670.
(47) Drouet, C. Apatite formation: why it may not work as planned, and how to conclusively identify apatite compounds. *BioMed. Res. Intl.* **2013**, *2013*, 1.
(48) Bhaskar, R.; Li, J.; Xu, L. A comparative study of particle size dependency of IR and XRD methods for quartz analysis. *Am. Ind. Hyg. Assoc. J.* **1994**, *55* (7), 605−609.
(49) Ferreira, A.; Oliveira, C.; Rocha, F. The different phases in the precipitation of dicalcium phosphate dihydrate. *J. Cryst. Growth* **2003**, *252* (4), 599−611.
(50) Boskey, A. L.; Posner, A. S. Conversion of amorphous calcium phosphate to microcrystalline hydroxyapatite. A pH-dependent, solution-mediated, solid-solid conversion. *J. Phys. Chem.* **1973**, *77* (19), 2313−2317.
(51) Reynaud, C.; Thomas, C.; Costentin, G. On the Comprehensive Precipitation of Hydroxyapatites Unraveled by a Combined Kinetic−Thermodynamic Approach. *Inorg. Chem.* **2022**, *61* (7), 3296−3308.
(52) Jo, M.-k.; Cho, Y. S.; Holló, G.; Choi, J.-M.; Lagzi, I.; Yang, S. H. Spatiotemporal and Microscopic Analyses of Asymmetric Liesegang Bands: Diffusion-Limited Crystallization of Calcium Phosphate in a Hydrogel. *Cryst. Growth Des.* **2021**, *21* (11), 6119−6128.
(53) Ruiz-Agudo, C.; Lutz, J.; Keckeis, P.; King, M.; Marx, A.; Gebauer, D. Ubiquitin Designer Proteins as a New Additive Generation toward Controlling Crystallization. *J. Am. Chem. Soc.* **2019**, *141* (31), 12240−12245.
(54) Seepma, S. j. Y.; Ruiz-Hernandez, S. E.; Nehrke, G.; Soetaert, K.; Philipse, A. P.; Kuipers, B. W.; Wolthers, M. Controlling $CaCO_3$ Particle Size with $\{Ca^{2+}\}$:$\{CO_3^{2-}\}$ Ratios in Aqueous Environments. *Cryst. Growth Des.* **2021**, *21* (3), 1576−1590.
(55) Amjad, Z.; Koutsoukos, P.; Tomson, M.; Nancollas, G. The growth of hydroxyapatite from solution. A new constant composition method. *J. Dent. Res.* **1979**, *58* (4), 1431−1432.
(56) Tomson, M.; Nancollas, G. Mineralization kinetics: a constant composition approach. *Science* **1978**, *200* (4345), 1059−1060.
(57) Gebauer, D.; Gale, J. D.; Cölfen, H. Crystal Nucleation and Growth of Inorganic Ionic Materials from Aqueous Solution: Selected Recent Developments, and Implications. *Small* **2022**, *18*, 2107735.
(58) Eyring, H. The activated complex and the absolute rate of chemical reactions. *Chem. Rev.* **1935**, *17* (1), 65−77.
(59) McDowell, H.; Gregory, T.; Brown, W. Solubility of $Ca_5(PO_4)_3OH$ in the System $Ca(OH)_2$-H_3PO_4-H_2O at 5, 15, 25, and 37 C. *J. Res. Natl. Bur. Stand., Sect. A* **1977**, *81A* (2−3), 273−281.
(60) Gregory, T. M.; Moreno, E. C.; Brown, W. E. Solubility of $CaHPO_4{\cdot}2H_2O$ in the system $Ca(OH)_2$-H_3PO_4-H_2O at 5, 15, 25, and 37.5° C. *J. Res. Natl.. Bur. Stand., Sect. A* **1970**, *74*, 461−475.
(61) Gebauer, D.; Kellermeier, M.; Gale, J. D.; Bergström, L.; Cölfen, H. Pre-nucleation clusters as solute precursors in crystallisation. *Chem. Soc. Rev.* **2014**, *43*, 2348−2371.

https://doi.org/10.1021/acs.cgd.3c00851
Cryst. Growth Des. 2023, 23, 7037−7043